WILEY | Hindawi

Research Article

Prediction of Surface Settlement Induced by Large-Diameter Shield Tunneling Based on Machine-Learning Algorithms

Chao Li [iD],[1,2,3] **Jinhui Li,**[1] **Zhongqi Shi** [iD],[2,4,5] **Li Li,**[2] **Mingxiong Li,**[1] **Dianqi Jin,**[2,4,5] **and Guo Dong**[1]

[1]*Department of Civil and Environmental Engineering, Harbin Institute of Technology (Shenzhen), Shenzhen 518055, China*
[2]*Shenzhen Urban Public Safety and Technology Institute, Shenzhen 518046, China*
[3]*Key Laboratory of Urban Safety Risk Monitoring and Early Warning, Ministry of Emergency Management,
 Shenzhen 518046, China*
[4]*Safe Urban Development Institute of Science and Technology (Shenzhen), Shenzhen 518046, China*
[5]*Shenzhen Key Laboratory of Urban Disasters Digital Twin, Shenzhen 518019, China*

Correspondence should be addressed to Chao Li; colin_lichao@163.com

The accurate prediction of surface settlement caused by large-diameter shield tunneling is crucial for the safety of the tunnel environment. However, due to the complexity and uncertainty of the rock-machine interaction and groundwater variation, it is difficult to predict the settlement by developing traditional theoretical methods. Recently, a big number of data obtained from the Chunfeng shield tunnel in China provides the possibility to predict the settlement using machine-learning methods. In this study, the equipment parameters, the geological parameters, and the monitored settlements are used to establish the models. Three machine-learning algorithms (i.e., long-short-term memory (LSTM), random forest (RF), and gated recurrent unit (GRU)) are used to predict the surface settlement. Three indicators, mean absolute error (MAE), accuracy (ACC), and coefficient of determination (R^2), are selected to evaluate the prediction performance. Results demonstrated that the filtering and selection of model parameters is vitally important to the accuracy of model prediction. Among the three machine-learning algorithms, the LSTM algorithm gives the best accuracy in predicting the maximum surface settlement and can effectively predict the settlement development in different strata.

1. Introduction

The increasing demand of urban underground space development has led to large-diameter shield application in large-scale tunnel construction [1]. In the process of large-diameter shield construction, it will inevitably disturb the surrounding strata and result in surface settlement, which may pose a threat to the safety of the surrounding environment [2–4]. Therefore, it is necessary to predict the surface settlement caused by shield construction.

The soil deformation is affected by complex rock-machine interaction. In addition, because the tunnel changes the hydraulic connection of groundwater, it is easy to produce water and soil loss and drainage consolidation, which further aggravates the surface settlement [5–8]. At present,

the prediction methods of soil settlement mainly include the empirical method [9–12], theoretical method [13–16], modeling method [17–21], and machine-learning method [22–25]. The empirical method has a simple calculation formula and convenient engineering application, but it is difficult to consider the influence of construction factors. The physical model of the theoretical method is clear, but it needs to meet the calculation assumptions, and the scope of application is limited. The modeling method establishes the model through numerical simulation and model test, but it can hardly simulate all the actual situations. The machine-learning method deeply excavates the internal potential laws of the data through the self-organizing learning and can consider a variety of internal and external factors at the same time [26], which provides an approach for

the prediction of surface settlement caused by shield tunnel construction.

In recent decades, with the development of statistical computing science, various machine-learning algorithms have been proposed and were widely used in tunneling-induced surface settlement prediction. Suwansawat and Einstein [27] used artificial neural networks to develop predictive relations between shield tunnel characteristics and surface deformation and proved that machine learning can become a useful predictive method. Pourtaghi and Lotfollahi-Yaghin [28] applied different wavelets as activation functions to predict the maximum surface settlement due to tunneling and indicated that using wavelets as ANN transfer functions can enhance the network efficiency. Kohestani et al. [29] used random forest (RF) for the prediction of maximum surface settlement caused by earth pressure balance shield tunneling; the proposed RF model shows a better performance than ANN. Chen et al. [30] approached the nonlinear relationship between maximum ground surface settlements and various parameters via the machine-learning method. Besides, other scholars have achieved outstanding research results [31–34], and the existing research results demonstrated that the machine-learning algorithm has great potential in surface subsidence prediction. However, the current research still has the following problems: (1) The existing studies mainly focus on ordinary-diameter metro shield tunnel, while there are few case studies on surface settlement caused by large-diameter shield construction. (2) The current researches are often limited to the prediction of the maximum surface settlement, while there is little prediction on the development process of surface settlement. (3) The existing prediction models generally adopt only one machine-learning algorithm; it is difficult to distinguish which algorithm is most suitable for surface subsidence prediction.

In this study, based on the big data of the Chunfeng large-diameter shield tunnel in China, three machine-learning algorithms were used to explore the prediction method of the maximum surface settlement. After optimization, the prediction model with the highest accuracy was proposed; then, the development of surface subsidence in different strata was predicted.

2. Database

The Chunfeng tunnel is located in the southeast of Shenzhen, China, as shown in Figure 1. The total length of the tunnel is 5.08 km, among which the shield tunnel section is 3.58 km, and the excavation diameter of the shield tunnel is 15.8 m. It was the largest diameter shield tunnel in China when the project started. The shield tunnel section passes through 29 old buildings, including densely populated areas such as Shenzhen Railway Station and Guangkun Hotel. Silt layer, permeable sand layer, and multiple fault zones are widely distributed along the line. In addition, Chunfeng tunnel is close to the Shenzhen River and Buji River; therefore, the surrounding strata have rich groundwater and a high seepage coefficient. In this situation, the large shield tunneling project very easily causes stratum deformation and

building damage. Therefore, it is necessary to predict the surface settlement and take control measures in time to avoid the possible risks caused by the induced settlement.

The shield section of Chunfeng tunnel starts from mileage K0+756 and has been excavated to mileage K2+100 so far, and the geological profile of this section is shown in Figure 2. The strata of the shield tunnel working face are mostly coarse-grained granite, cataclastic rock, tuffaceous sandstone, schist, metamorphic sandstone, breccia, and mylonite. There are 9 fault zones with different shapes and sizes distributed along the line. Special strata mainly include the artificial fill layer, muddy cohesive soft soil, weathered rock, and geological fault. The maximum uniaxial compressive strength of rock reaches 141.44 MPa. Strong permeable layers such as medium sand, gravel sand, and pebble are locally distributed, and the biggest permeability coefficient reaches 30 m/d.

The factors relevant to shield tunneling-induced surface settlement can be classified into equipment parameters, geological parameters, and geometric parameters [30]. In the process of shield tunneling, the big data was measured automatically by the shield machine, 132 kinds of equipment parameters were recorded per second, and 16 kinds of corresponding geological parameters and one geometric parameter were also collected in this project. Some equipment parameters, geological parameters, and geometric parameter are shown in Table 1. The accuracy of surface settlement monitoring reaches millimeter level. Data were recorded at the same time every day. Monitoring points were arranged along the line above the middle axis of the shield, and the monitoring work continued until the stratum is stable.

3. Machine-Learning Algorithms

3.1. Long-Short-Term Memory (LSTM) Algorithm. The LSTM algorithm is a special type of RNN (Recurrent Neural Network), which can learn long-term dependent information, and is suitable for processing and predicting important events with relatively long interval and delay in time series [35]. The LSTM algorithm introduces the function of "gate operation" and adds three control units: an input layer, one or several hidden layer(s), and an output layer; it can change the cumulative multiplication in the gradient into accumulation, which solves the problem of the vanishing gradient. When the information is inputted to the LSTM algorithm, control units will judge the information, the information that conforms to the rules will be left, or it will be forgotten. By selectively remembering the effective information, the problem of long sequence dependence in the neural network can be solved. The input gate controls the input activation flow of the storage unit. The forgetting gate controls whether the information in the previous step is remembered or forgotten. The output gate is responsible for transmitting useful information to the next memory block [36]. Based on the characteristics of the LSTM model delay unit and feedback structure, the time series array can be established by using the duration data of the surface settlement at engineering measuring points, and the surface
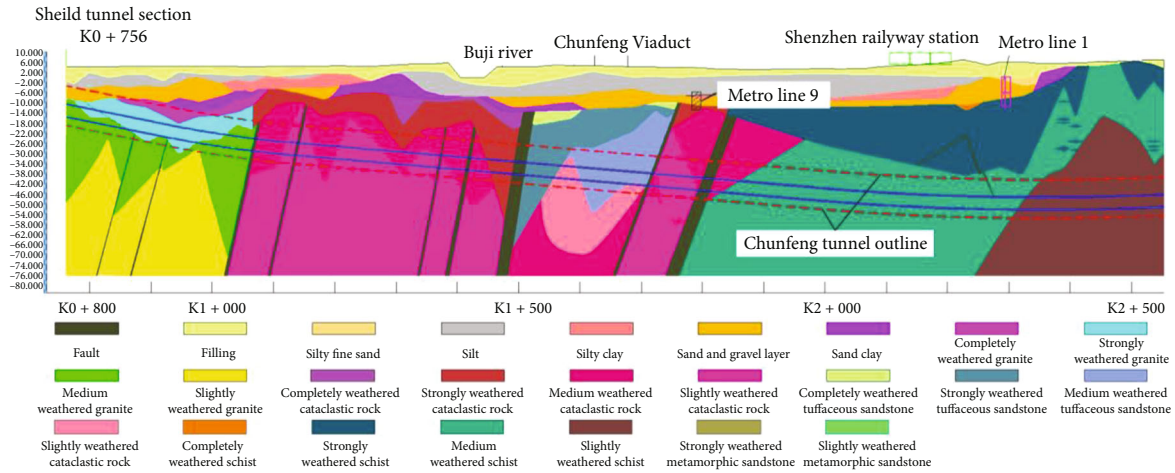
Figure 1: Chunfeng tunnel plan.

Figure 2: Chunfeng tunnel geological profile.

Table 1: Parameters of the project.

Data	Type	Variable
Input	Equipment parameter	Cutter torque, cutter rotation speed, propulsion speed, penetration, total thrust, cutter extrusion force, roll angle, slope angle, shield tail deviation, notch deviation, guide mileage, propel cylinder stroke difference, top pressure of slurry silo, air cushion chamber pressure, slurry inflow, sludge discharge, slurry inlet density, sludge density, outlet pressure of sludge inlet pump, suction pressure of sludge inlet pump, inlet pressure of slurry discharge pump, etc. (132 in total)
	Geological parameter	Natural moisture content, natural density, uniaxial compressive strength, modulus of elasticity, void ratio, cohesion, internal friction angle, organic matter content, SPT blow count, permeability coefficient, groundwater level, specific gravity, liquid limit, plastic limit, compression modulus, compressibility coefficient (16 in total)
	Geometric parameter	Cover depth
Output	Settlement parameter	Maximum surface settlement

settlement at the measuring points along the tunnel can be predicted.

3.2. Gated Recurrent Unit (GRU) Algorithm. The GRU algorithm is a special type of RNN. GRU was also proposed to solve the problems of the gradient in long-term memory and backpropagation like LSTM. It combines the forgetting gate and input gate into a separate update gate, combines the cell state and hidden state, and makes some other changes to make its model simpler than the standard LSTM model. The GRU algorithm uses the update gate and reset gate to solve the problem of the vanishing gradient [37]. The reset gate determines how to combine the new input with the previous memory, and the update gate determines how many previous memories work.

3.3. Random Forest (RF) Algorithm. The RF algorithm is an integrated method based on the decision tree first developed by Breiman [38]. The random forest randomly extracts some samples from the original samples to generate a new sample

set by putting them back. Repeat this operation to generate multiple sample sets, and each sample set will generate a decision tree. In the process of generating each decision tree, when each node branches, some features are randomly selected to participate in the branches of the decision tree and then recursive branches. In the process of recursive branches, some features are randomly selected from the remaining features each time. Then, multiple decision trees will be generated. When predicting the category of new input samples, each tree will produce a prediction result. Finally, the category of new input samples will be determined via the principle of minority obeying majority [39].

4. Prediction of Maximum Surface Settlement

4.1. Prediction Model. The prediction model needs to consider the impact of various parameters on surface settlement during shield tunneling. The maximum surface settlements along the tunnel are taken as output parameters, and the corresponding equipment parameters, geological parameters, and geometric parameters are selected as input parameters. Through the training sample data, the network structure and relevant learning parameters are determined, and a multi-input and single-output nonlinear prediction model is established to realize the prediction of the maximum surface settlement along the tunnel. According to the completed part of the shield tunneling, 446 groups of data have been obtained, of which 376 groups are used for model training and 70 groups for surface settlement prediction and verification.

4.1.1. Original Model of All Parameters. Considering all 132 equipment parameters, 16 geological parameters, and a geometry parameter, the 149 kinds of parameters are taken as the input parameters to set up the model.

4.1.2. Optimized Model of Filtered Parameters. In the actual engineering prediction, it is impossible to consider all the 149 influence parameters. On the one hand, too much field data collection leads to low prediction efficiency. On the other hand, too many parameters will complicate the construction of the neural network model and greatly prolong the training time. Meanwhile, the parameters are not independent of each other, considering that all parameters may lead to overfitting, which will reduce the accuracy of model prediction. Therefore, some parameters need to be eliminated.

(1) Constant Attribute Parameter Filtering. Some of the 149 parameters are constant values, such as tunnel diameter and tunneling mode; filter out these constant parameters firstly. Besides, the parameters that vary very little, such as scouring flow of crusher and suction pressure of sludge pump, need to be filtered out.

(2) Highly Correlated Parameter Filtering. The parameters that are strongly dependent on another parameter, which provide little new information, will reduce the efficiency of the model. The highly correlated parameters were identified by the Pearson correlation coefficient. The Pearson correlation coefficient [40] is calculated as follows:

$$r_{xy} = \frac{n\sum x_i y_i - \sum x_i \sum y_i}{\sqrt{n\sum x_i^2 - (\sum x_i)^2}\sqrt{n\sum y_i^2 - (\sum y_i)^2}}, \quad (1)$$

where r_{xy} is the Pearson correlation coefficient between parameter x and parameter y and i takes 1, 2,…, n in sequence.

When the Pearson correlation coefficient between two parameters is larger than 0.9, it means that the information contained in the two parameters is highly similar. For example, the correlation coefficients between cylinder thrusts of groups A~F in the propulsion system are greater than 0.9, indicating that they are highly correlated parameters, so only one of them can be retained.

After filtering out the constant attribute parameters and highly correlated parameters, 34 parameters are retained.

4.1.3. Optimized Model of RF Key Parameters. RF is an ensemble algorithm based on the decision tree. Through RF, the importance of each parameter to the prediction results can be evaluated. The bagging method was used to randomly extract 50 data sets from the original data, and each data set was inputted to the decision tree. By comparing the variable importance measure (VIM) of the Gini index calculated by the decision tree, the importance evaluation of each parameter is realized.

The Gini index (GI) is the probability of a randomly selected parameter being misclassified in a data set [31], and the Gini index of parameters is calculated by

$$GI_m = \sum_{j=1}^{k} p_j\left(1 - p_j\right), \quad (2)$$

where GI_m expresses the Gini index of the node N_m, p_j represents the probability of the jth parameter being classified into the data set of node N_m, and k is the number of parameters in the data set.

The VIM of the jth parameter of the node N_m is calculated as Equation (3), which represents the change of the Gini index after splitting. The VIM of the jth parameter in the decision tree T_i is the sum of VIM for each node that the jth parameters appeared, which is calculated via Equation (4). The VIM of the jth parameter in the random forest is calculated via Equation (5), which means the sum of the VIM of each decision tree [31].

$$VIM_{j,m}^{Gini} = GI_m - GI_l - GI_r, \quad (3)$$

$$VIM_{j,i}^{Gini} = \sum_{m \in M} VIM_{j,m}^{Gini}, \quad (4)$$

$$VIM_j^{Gini} = \sum_{i=1}^{n} VIM_{j,i}^{Gini}, \quad (5)$$

where $\text{VIM}_{j,m}^{\text{Gini}}$ represents the VIM of the jth parameter in the node N_m, GI_m means the Gini index at node N_m, GI_l and GI_r are the Gini indexes after splitting, $\text{VIM}_{j,i}^{\text{Gini}}$ expresses the VIM of the jth parameter in the decision tree T_i, M is the node set of the jth parameters appearing, $\text{VIM}_j^{\text{Gini}}$ is the VIM of the jth parameter in the random forest, and n is the number of decide trees in a random forest.

By selecting different numbers of parameters that have the most significant impact on the surface settlement prediction, the input parameters of the neural network model are further reduced, and then, the prediction model is optimized to improve the prediction accuracy of surface settlement. After optimization, the epoch, batch size, and learning rate were taken as 3000, 25, and 0.003, respectively.

4.2. Performance Evaluation Method. Performance evaluation is generally conducted to assess the applicability and practicality of the model. In this paper, coefficient of determination (R^2), mean absolute error (MAE), and the customization performance indicator accuracy (ACC) are selected to demonstrate the correspondence between predictions and measurements [30]. The equations of R^2, MAE, and ACC are as follows:

$$R^2 = 1 - \frac{\sum_{i=1}^{N}(y_i - \widehat{y}_i)^2}{\sum_{i=1}^{N}(y_i - \bar{y})^2}, \tag{6}$$

$$\text{MAE} = \frac{1}{N}\sum_{i=1}^{N}|y_i - \widehat{y}_i|, \tag{7}$$

$$\text{ACC} = \frac{N_i}{N} \times 100\%, \tag{8}$$

where y_i is the measured value, $\widehat{y}_i$ is the predicted value, $\bar{y}$ is the average of measured values, N_i is the number of correct predictions $\widehat{y}_i$, and N is the number of predictions.

In Equation (6), the denominator represents the dispersion of the measured value, and the numerator represents the error between the measured value and the predicted value. Therefore, R^2 eliminates the influence of the dispersion of the original data on the predicted value. The closer the value is to 1, the better the model fitting is. Generally, the prediction fitting is acceptable when R^2 is larger than 0.4. MAE indicates the error between the predicted value and the measured value. ACC is the ratio of the accurate prediction number to the total prediction number. According to the actual monitoring needs of the project, it is defined that the prediction is accurate if the error between the predicted value and the measured value is less than 2 mm.

5. Results

According to different models and different input parameters, the predicted 70 groups of validation data are analyzed as follows. The prediction model construction and optimization process of the three machine-learning algorithms are similar. Due to space limitations, the prediction processes of the three algorithms are not all described in detail, and only the LSTM model with the highest accuracy was selected as the typical case to illustrate the model construction process and result analysis.

5.1. Prediction of Original Model with All Parameters. Considering all 149 parameters, the prediction results obtained by the LSTM algorithm model is shown in Figure 3.

With the full parameters, the prediction accuracy is 64.3%, and the prediction results of some groups are not accurate enough. The R^2 value is 0.64, which indicates that the development trend of prediction results is acceptable. The MAE value is 1.59 mm; the value is okay but there are large errors in the prediction results of some groups. The overall prediction performance is not good enough.

5.2. Prediction of Optimized Model with Filtered Parameters. 34 parameters are retained after filtering out the constant attribute parameters and highly correlated parameters. Considering the retained 34 parameters, the prediction results obtained by the LSTM algorithm model is shown in Figure 4.

After parameter filtering, the ACC is significantly improved from 64.3% to 84.3%, and MAE is evidently reduced to 0.91 mm. On the whole, the predicted data are consistent with the measured data; however, the surface settlement of some sections has nonnegligible errors, such as groups 20~30 and groups 50~65. That is because of the predictive model as well as the tunnel environment. It is found that the tunnel passed through the Baoan overpass at the location of groups 20~30, and the daily traffic flow had a certain impact on the surface settlement. The location of groups 50-65 is close to Buji River, and the flow of groundwater has a significant impact on surface settlement.

5.3. Prediction of Optimized Model with RF Key Parameters. The corresponding importance of the filtered 34 parameters is analyzed via RF algorithm, and the results are shown in Figure 5. According to the importance analysis, the grouting pressure is the most important parameter. That is because the grouting pressure directly affects the compactness of the surrounding soil of the tunnel, thus affecting the formation deformation and the surface settlement. The slurry sump pressure is the second important parameter since it determines the stress state of the excavation surface, which affects the surface settlement in front of the shield. The above analysis illustrates that the RF importance analysis results are reasonable.

Through parameter-filtering analysis, it can be seen that the selection of parameters has an important impact on the prediction of surface settlement, and excessive redundancy of parameters has an adverse impact on the prediction accuracy. Therefore, based on the analysis results of the importance of each parameter from the RF algorithm, gradually reduce the number of parameters by removing relatively unimportant parameters. The prediction accuracy of surface settlement with different numbers of parameters is obtained, as shown in Figure 6.
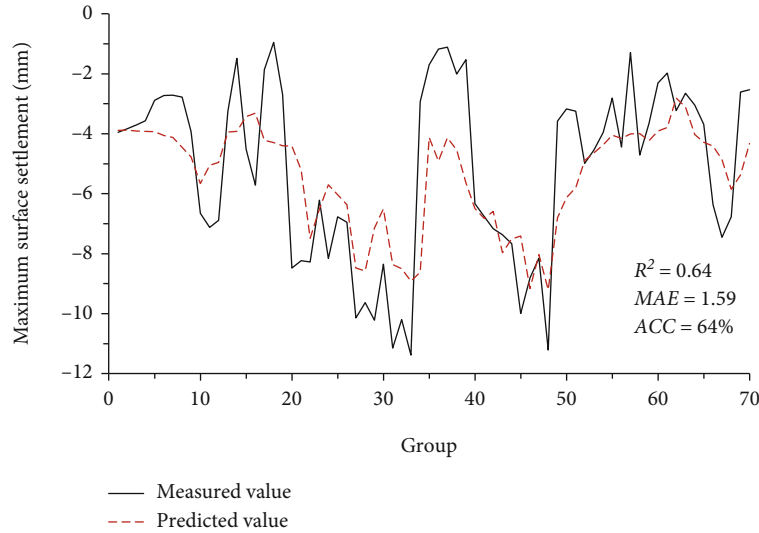
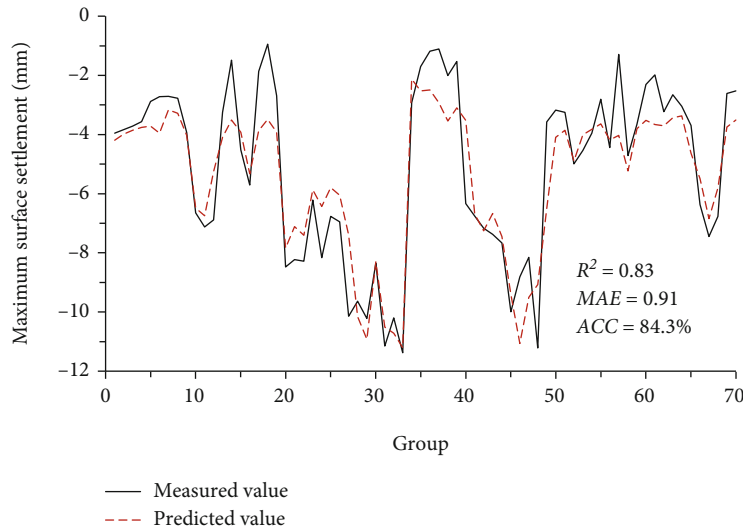FIGURE 3: Prediction of original model with all parameters.

FIGURE 4: Prediction of optimized model with filtered parameters.

It can be seen from Figure 6 that the accuracy of surface settlement prediction can be improved through adjusting the input parameters selected by importance. When the most important 16 parameters are selected as input parameters, the accuracy of the prediction obtained by the LSTM algorithm model is the highest, reaching 92.9%, and the MAE value was less than 1 mm, as shown in Figure 7. In this prediction model, 16 input parameters include 13 equipment parameters, 2 geological parameters, and 1 geometric parameter. This illustrated that the setting of equipment parameters was vital to control shield tunneling-induced surface settlement. The results indicate that the random forest is an effective way to identify the most important factors, enhance the data efficiency, and improve model accuracy.

5.4. Prediction Comparison of Different Algorithms. After model input parameter filtering and key parameter optimization, LSTM, GRU, and RF algorithms are used for predic-tion. The comparison curves of prediction results are shown in Figure 8. According to the curve distribution, the three algorithms can predict the surface subsidence well, among which the predicted results of LSTM and GRU algorithms are more consistent with the measured value.

Comparing the three evaluation indicators, as shown in Table 2, the R^2 values of LSTM and GRU algorithms are both 0.86, and the RF algorithm's R^2 value is 0.81, which is slightly lower than the other two algorithms. The MAE values of the LSTM and GRU algorithms are both lower than 1 mm, while the RF algorithm's MAE value is slightly higher than 1 mm. In terms of ACC, the LSTM algorithm is the highest, the GRU algorithm is slightly lower, and the RF algorithm is the lowest. Overall, ACC values of three algorithms are all higher than 80%. Among them, the prediction performances of LSTM and GRU are better, while the RF prediction performance is relatively backward.
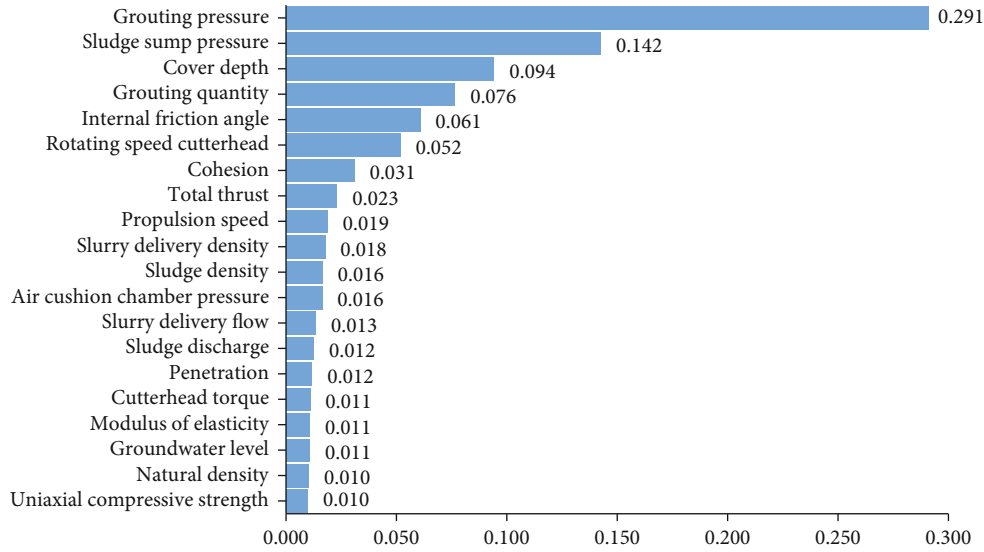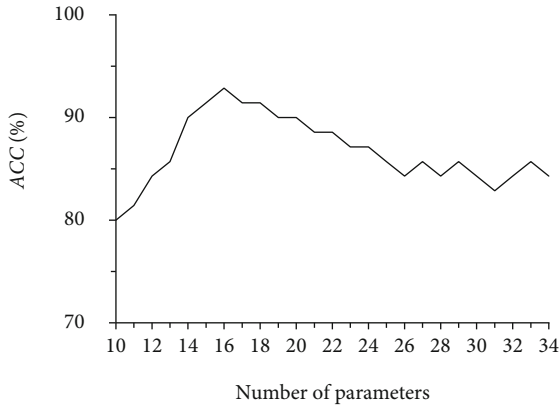
Figure 5: The VIM of key parameters.

Figure 6: The prediction accuracy with different numbers of parameters.

6. Prediction of Surface Subsidence Development

6.1. Analysis of Surface Settlement Development Characteristics. The surface settlement monitoring time of the Chunfeng tunnel covers three stages: the shield machine excavating close to the monitoring point, passing through the monitoring point, and driving away from the monitoring point, and the monitoring stopped when the surface settlement value tends to be stable. The monitoring period of each point varies from 60 to 110 days.

Before predicting the development of surface settlement along the tunnel, select the representative point DBC-1058 (located at the tunnel mileage of 1058 m above the central axis of the tunnel), analyze the measured surface settlement value to reveal the regional surface settlement development characteristics of Chunfeng tunnel, and provide a comparison basis for the prediction results. The variation curve of surface settlement at point DBC-1058 is shown in Figure 9. When the shield machine was directly below the monitoring point, the corresponding date is day 0.

It can be seen from the curve in Figure 9 that the surface settlement development in the process of shield tunneling can be divided into three periods.

(1) *Initial period.* The shield has not reached the monitoring point, but the cutterhead and the slurry have a certain squeezing effect on the front stratum. When the squeezing force is greater than the in situ stress, it will cause the uplift of the front stratum; otherwise, it will produce settlement. In this period, as the shield machine has not yet arrived, the change of the ground surface at the monitoring point is small.

(2) *Crossing period.* When the shield machine passes through the monitoring point, the in situ stress under the monitoring point is released, and there are inevitable pores between the shield and surrounding soil, resulting in rapid surface settlement.

(3) *Consolidation period.* Due to the shrinkage of slurry and the conduction of previous pores, there is still a certain surface settlement in this period. Then, the soil gradually consolidates and tends to be stable. In the process of surface settlement monitoring, considering the structural construction, trolley operation, and measurement errors in the tunnel, there are slight fluctuations in the surface settlement monitoring value.

The settlement characteristics of monitoring point DBC-1058 was consistent with the engineering practice and belonged to the classic settlement law, which show that the data resources collected in this project were reasonable.

6.2. Prediction Model. According to the conclusion in Section 4, based on the LSTM algorithm, select the most important 16 parameters as input parameters; the prediction model has the highest accuracy in predicting surface
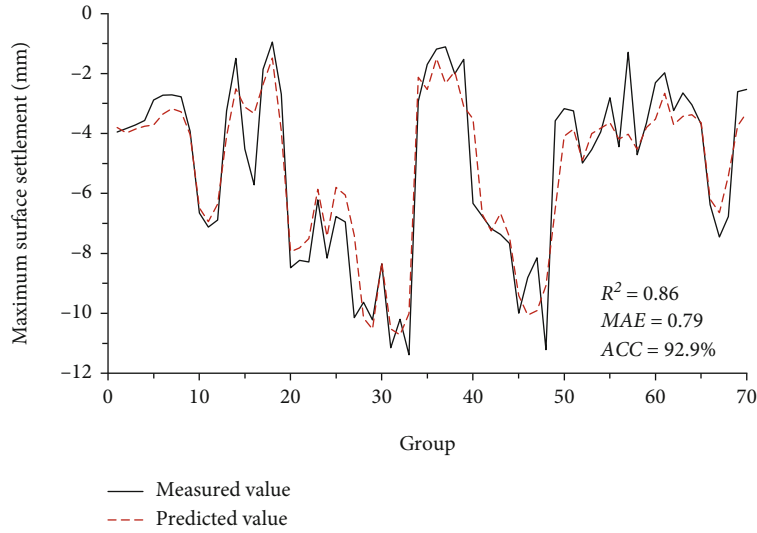
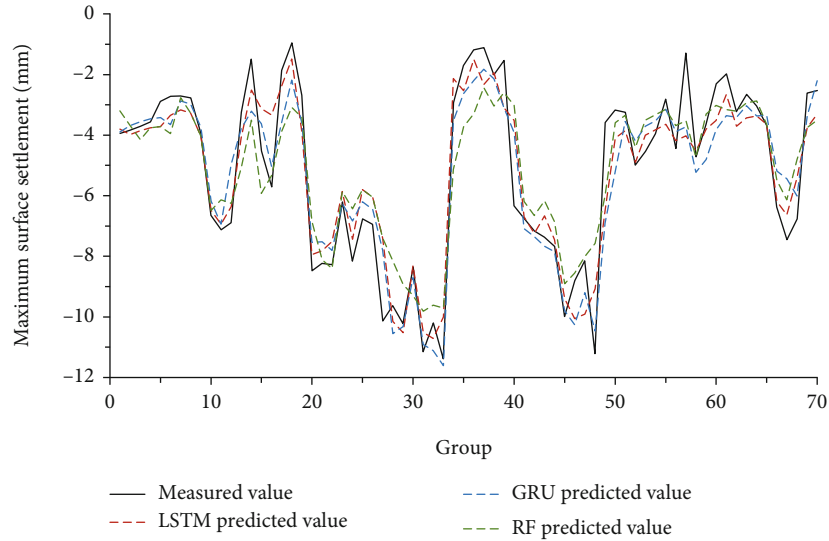FIGURE 7: Prediction of optimized model with RF key parameters.

FIGURE 8: Comparison of prediction results of different algorithms.

TABLE 2: Comparison of prediction indicators of different algorithms.

Algorithm	R^2	MAE	ACC
LSTM	0.86	0.79	92.9%
GRU	0.86	0.81	91.4%
RF	0.81	1.02	84.3%

settlement. Therefore, this section selects the most important 16 parameters in Figure 6 plus time parameters (the day when the shield machine passed through this monitoring point is day 0) as input parameters. The corresponding surface settlement variation compared with that of day 0 is the output parameter. The input and output parameters of the model are shown in Table 3.

Among the existing 446 groups of settlement data, each group includes the surface settlement value development of the whole periods. Generally, the monitoring lasted for more than 45 days after the shield machine passes through. In order to predict the development of the surface settlement after the shield machine passes through, a model was established based on 446 groups of settlement development data (376 groups for training and 70 groups for prediction). By predicting the variation of the corresponding surface settlement (compared with day 0) in different days after the shield crossing, the 45-day development curve of the surface settlement at each monitoring point is obtained. After 45 days, most monitoring points have entered the final settlement stability period, so the curves can reflect the diachronic development law of surface settlement after shield passing and reflect the impact of shield excavation on surface settlement.
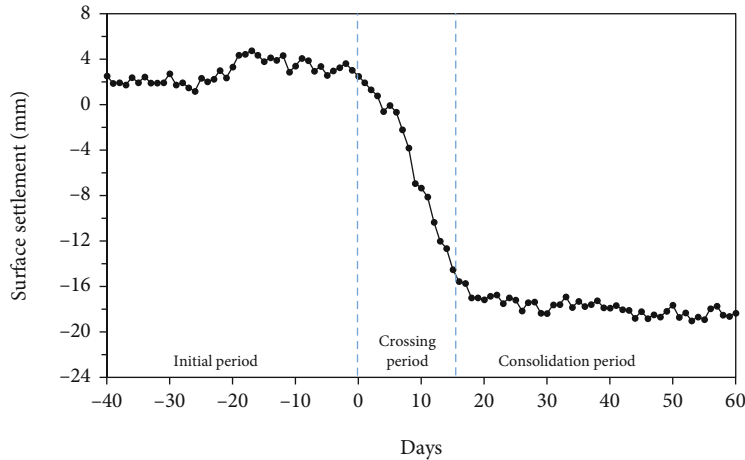
FIGURE 9: Variation curve of surface settlement at point DBC-1058.

TABLE 3: Parameters of the prediction model.

Data	Type	Variable
Input	Equipment parameter	Grouting pressure, sludge sump pressure, grouting quantity, rotating speed cutterhead, total thrust, propulsion speed, slurry delivery density, sludge density, air cushion chamber pressure, slurry delivery flow, sludge discharge, penetration, cutterhead torque (13 in total)
	Geological parameter	Internal friction angle, cohesion
	Geometric parameter	Cover depth
	Date parameter	Date
Output	Settlement parameter	Surface settlement variation

6.3. Results. Through the above basic data and LSTM algorithm, 70 groups of surface settlement values in different days were predicted, and then, combining different days' settlement values at each monitoring point, the 70 groups of surface settlement in 45 days after shield crossing were obtained. In order to evaluate the prediction performance, R^2, ACC, and MAE are selected as evaluation indicators.

The performance evaluation of the predicted results of 70 groups is shown in Table 4. The average value of R^2 is 0.73, indicating that the change trends of the predicted results are consistent with the measured results. The average value of ACC is 77.4%, which means the overall prediction accuracy is high. The average value of MAE is 1.95 mm, and the errors are acceptable. As different monitoring points are affected by different geological environment and construction conditions, the performances of prediction results are also different. The accuracy of some monitoring points is very high, while the accuracy of some monitoring points needs to be improved. In general, the prediction performance meets the needs of guiding field data analysis.

After stratum analysis, 70 groups of prediction points can be roughly divided into four categories according to the stratum of tunnel crossing: (1) medium and slightly weathered rock mixed with fracture zone stratum, (2) upper soft and lower hard strata (the upper part is medium weathered sandstone and the lower part is slightly weathered sandstone), (3) uneven on the left and right strata (there are two

TABLE 4: Performance evaluation of prediction results of 70 groups.

Evaluation indicator	Maximum value	Minimum value	Average value
R^2	0.93	0.48	0.73
ACC	91.1%	64.4%	77.4%
MAE (mm)	4.17	0.65	1.95

different lithologic strata on the left and right, mainly tuffaceous sandstone and fracture zone), and (4) completely slightly weathered slate. Next, the typical surface settlement development curves in four strata are selected to illustrate the settlement development characteristics. The surface settlement curves of typical monitoring points DBC-1625, DBC-1735, DBC-1927, and DBC-2120 of four corresponding strata are shown in Figure 10.

6.3.1. Medium and Slightly Weathered Rock Mixed with Fracture Zone Stratum. The monitoring time of point DBC-1625 lasted 87 days. When the shield machine reached this point, the surface settlement value was 1.20 mm as show in Figure 10(a), and the surface is slightly uplifted. From the perspective of surface settlement development, after the shield machine passed through the point, the surface settlement decreased rapidly. When the stratum was stable, the settlement value fluctuated around -24 mm. Due to the

(a) Typical prediction results in medium and slightly weathered rock mixed with fracture zone stratum

(b) Typical prediction results in upper soft and lower hard strata

(c) Uneven typical prediction results on the left and right strata

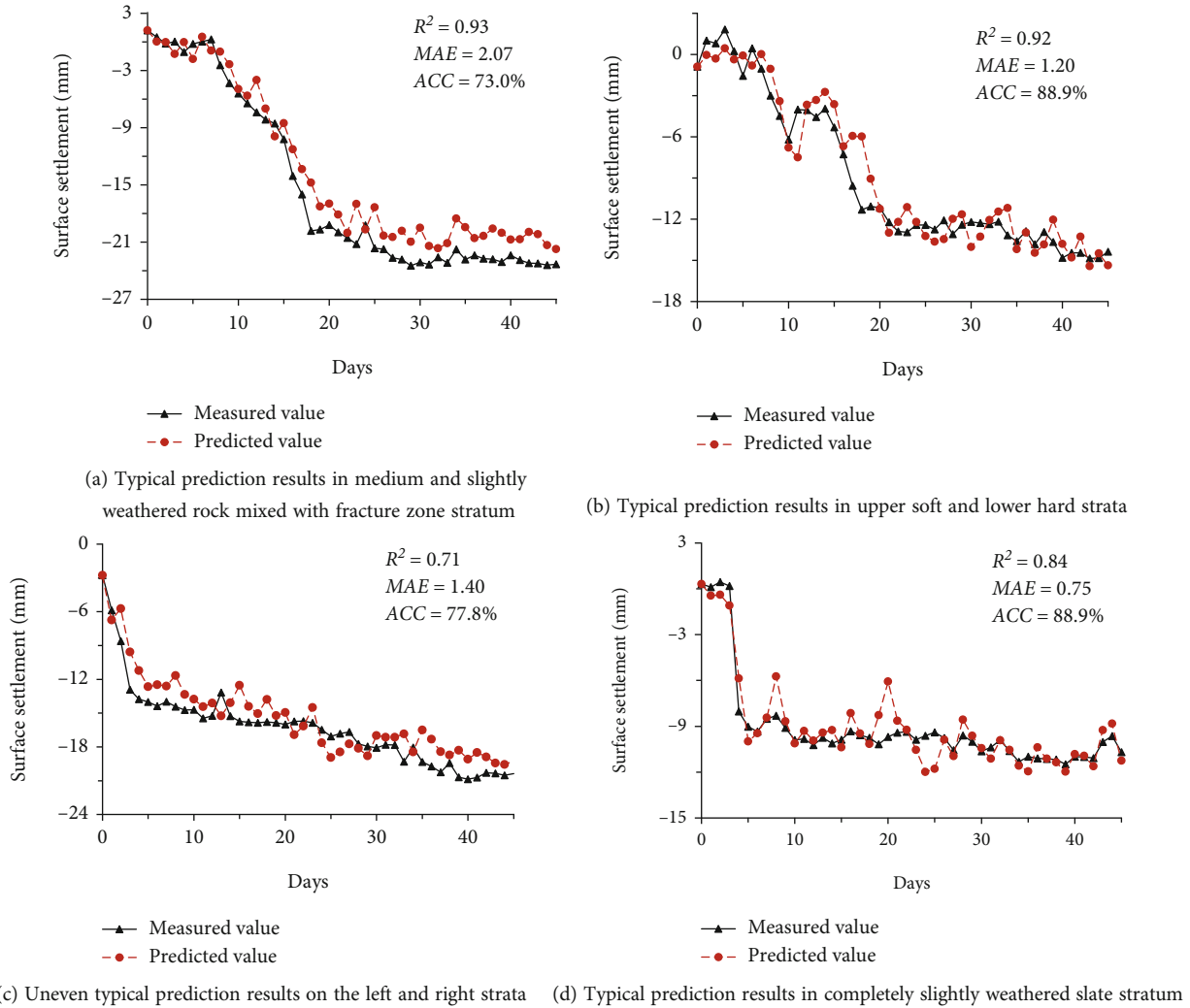(d) Typical prediction results in completely slightly weathered slate stratum

FIGURE 10: Comparison of typical prediction results of surface settlement development in different strata.

fracture zone, the final surface settlement was large. From the perspective of predicted performance of surface subsidence, the value of R^2 reached 0.93, indicating that the change trend of the predicted results was highly consistent with the measured results. However, when the stratum was basically stable, there was a slight gap between the predicted value and the measured value, resulting in a relatively large MAE value of 2.07 mm.

6.3.2. Upper Soft and Lower Hard Strata. The monitoring time of point DBC-1735 lasted 91 days. As show in Figure 10(b), when the shield machine reached this point, the surface settlement value was -0.9 mm, and no large settlement occurred. After rapid settlement, the final surface settlement value was stable around -14 mm. The variation trend of the predicted value was in good agreement with the measured value; the R^2 value reached 0.92. The accuracy of the model was very high, reaching 88.9%. The error was also controlled in a small range, and the MAE value was

1.2 mm. Overall, the prediction performance was good in upper soft and lower hard strata.

It is worth noting that the surface settlement on the 11th day increased significantly; that is because the stratum was sensitive and secondary grouting was carried out after the shield passed to prevent excessive surface settlement.

6.3.3. Uneven on the Left and Right Strata. As shown in Figure 10(c), when the shield machine reached point DBC-1927, the surface settlement value was -2.77 mm. It illustrated that the excavation before this point has caused a certain settlement. From the perspective of the surface subsidence development, after the shield machine passed through the point, the surface settlement decreased rapidly within 5 days then tended to decrease slowly, and the final surface settlement value fluctuated around -18 mm. From the perspective of predicted performance of surface subsidence, the value of R^2 was 0.71, which was lower than that of point DBC-1625 and DBC-1735. The MAE value was 1.4 mm and

the ACC value was 77.8%, and the predictive value and measured value fluctuated around the same datum line.

6.3.4. Completely Slightly Weathered Slate Stratum. Figure 10(d) shows the surface settlement development in completely slightly weathered slate. When the shield machine reached point DBC-2120, the surface settlement value was 0.31 mm, and it was stable in the initial period. After the shield machine passed through the point, the surface settlement decreased rapidly within 4 days then tended to become stable. The value of R^2 was 0.84; the fitting effect was good. The MAE value was 0.75 mm, which was the smallest prediction error among the four points. The ACC value was high, reaching 88.9%. In general, due to the good stability of slightly weathered slate, there are less uncertain factors, and the model can predict the development of surface subsidence well.

To sum up, the prediction model considering time factors proposed in this paper can predict the surface subsidence development in different strata with high accuracy and small error overall, and the prediction results of the settlement development law accord with the strata characteristic, which can provide guidance for the development and control of surface subsidence in similar strata during the subsequent construction of the project.

7. Conclusion

Based on the big data of the Chunfeng large-diameter shield tunnel, this paper explores the use of machine-learning algorithms to predict the maximum value and development of surface settlement caused by shield tunneling. The following conclusions can be obtained:

(1) The accuracy of the maximum surface settlement prediction can be significantly improved by model parameter filtering and importance analysis. By filtering the constant, low variation, and high correlation parameters, the accuracy of the LSTM algorithm model was improved from 64% to 84.3%. Besides, a RF algorithm was used to analyze the importance of each input parameter. The model accuracy was further improved to 92.9% after further filtering of parameters based on importance

(2) LSTM, GRU, and RF algorithms are all applicable to the prediction of maximum surface settlement. Among them, LSTM and GRU have similar prediction performance with high accuracy, while the RF algorithm has a relatively lower prediction accuracy. Comparing the optimized prediction models of the three algorithms, the accuracy of the LSTM algorithm with the most important 16 parameters as the input parameters is the highest

(3) The development of the surface settlement with time was obtained using the LSTM algorithm. The prediction curve was basically consistent with the classical settlement development trend, which illustrated the rationality of the prediction model. The statistics of the prediction results show that the average accuracy

was 77.4% and the average error was within 2 mm. In general, the prediction performance satisfies the needs of engineering practice in the field

(4) The predicted results can reflect the characteristics of surface settlement development in different strata. The prediction model proposed in this paper provides guidance for the control of surface settlement during the subsequent construction of the project and provides a reference method for surface settlement prediction of other large-diameter shield tunneling projects

Data Availability

The data used to support the findings of this study are available from the corresponding author upon request.

Conflicts of Interest

The authors declare that they have no conflicts of interest.

Authors' Contributions

C. L. analyzed the data and wrote the manuscript; M. L. and D. G. collated the data and established the predictive model; J. L. and Z. S. proposed the research method; and D. J. and L. L. reviewed and edited the manuscript. All authors have read and agreed to the published version of the manuscript.

References

[1] X. Xie, Y. Yang, and M. Ji, "Analysis of ground surface settlement induced by the construction of a large-diameter shield-driven tunnel in Shanghai, China," *Tunnelling and Underground Space Technology incorporating Trenchless Technology Research*, vol. 51, no. 51, pp. 120–132, 2016.

[2] G. Zheng, T. Cui, X. Cheng et al., "Study of the collapse mechanism of shield tunnels due to the failure of segments in sandy ground," *Engineering Failure Analysis*, vol. 79, pp. 464–490, 2017.

[3] Q. Huang, H. Huang, B. Ye, D. Zhang, and F. Zhang, "Evaluation of train-induced settlement for metro tunnel in saturated clay based on an elastoplastic constitutive model," *Underground Space*, vol. 3, no. 2, pp. 109–124, 2018.

[4] S. L. Shen, H. N. Wu, Y. J. Cui, and Z. Y. Yin, "Long-term settlement behaviour of metro tunnels in the soft deposits of Shanghai," *Tunnelling and Underground Space Technology*, vol. 40, pp. 309–323, 2014.

[5] B. Bai and T. Li, "Irreversible consolidation problem of a saturated porothermoelastic spherical body with a spherical

cavity," *Applied Mathematical Modelling*, vol. 37, no. 4, pp. 1973–1982, 2013.

[6] B. Bai, L. Guo, and S. Han, "Pore pressure and consolidation of saturated silty clay induced by progressively heating/cooling," *Mechanics of Materials*, vol. 75, pp. 84–94, 2014.

[7] B. Bai and X. Shi, "Experimental study on the consolidation of saturated silty clay subjected to cyclic thermal loading," *Geomechanics and Engineering*, vol. 12, no. 4, pp. 707–721, 2017.

[8] B. Bai, R. Zhou, G. Cai, W. Hu, and G. Yang, "Coupled thermo-hydro-mechanical mechanism in view of the soil particle rearrangement of granular thermodynamics," *Computers and Geotechnics*, vol. 137, no. 8, article 104272, 2021.

[9] R. B. Peck, "Deep excavations and tunneling in soft ground," in *State of the Art Report. 7th International Conference on Soil Mechanics and Foundation Engineering*, pp. 255–290, Mexico, 1969.

[10] H. M. Hughes, "The relative cuttability of coal-measures stone," *Mining Science and Technology*, vol. 3, no. 2, pp. 95–109, 1986.

[11] J. K. Hamidi, K. Shahriar, B. Rezai, and J. Rostami, "Performance prediction of hard rock TBM using rock mass rating (RMR) system," *Tunneling and Underground Space Technology Incorporating Trenchless Technology Research*, vol. 25, no. 4, pp. 333–345, 2010.

[12] A. T. C. Goh, W. G. Zhang, Y. M. Zhang, Y. Xiao, and Y. Z. Xiang, "Determination of earth pressure balance tunnel-related maximum surface settlement: a multivariate adaptive regression splines approach," *Bulletin of Engineering Geology and the Environment*, vol. 77, no. 2, pp. 489–500, 2018.

[13] L. Ozdemir, *Development of theoretical equations for predicting tunnel boring ability*, Colorado School of Mines, 1977.

[14] D. Resendiz and M. P. Rome, *Settlement upon soft ground tunneling: theoretical solution*, pp. 65–74, 1981.

[15] B. Bai, "Fluctuation responses of saturated porous media subjected to cyclic thermal loading," *Computers and Geotechnics*, vol. 33, no. 8, pp. 396–403, 2006.

[16] B. Bai, Q. Nie, Y. Zhang, X. Wang, and W. Hu, "Cotransport of heavy metals and SiO_2 particles at different temperatures by seepage," *Journal of Hydrology*, vol. 597, article 125771, 2021.

[17] K. M. Lee and R. K. Rowe, "Subsidence owing to tunnelling. II. Evaluation of a prediction technique," *Canadian Geotechnical Journal*, vol. 29, no. 6, pp. 941–954, 1992.

[18] B. X. Yuan, Z. H. Li, Z. L. Su, Q. Z. Luo, M. J. Chen, and Z. Q. Zhao, "Sensitivity of multistage fill slope based on finite element model," *Advances in Civil Engineering*, vol. 2021, 13 pages, 2021.

[19] B. X. Yuan, Z. H. Li, Z. Q. Zhao, H. Ni, Z. L. Su, and Z. J. Li, "Experimental study of displacement field of layered soils surrounding laterally loaded pile based on transparent soil," *Journal of Soils and Sediments*, vol. 21, no. 9, pp. 3072–3083, 2021.

[20] B. X. Yuan, Z. H. Li, Y. M. Chen et al., "Mechanical and microstructural properties of recycling granite residual soil reinforced with glass fiber and liquid-modified polyvinyl alcohol polymer," *Chemosphere*, vol. 286, article 131652, 2022.

[21] B. Bai, G. C. Yang, T. Li, and G. S. Yang, "A thermodynamic constitutive model with temperature effect based on particle rearrangement for geomaterials," *Mechanics of Materials*, vol. 139, article 103180, 2019.

[22] J. S. Chou and C. Lin, "Predicting disputes in public-private partnership projects: classification and ensemble models," *Journal of Computing in Civil Engineering*, vol. 27, no. 1, pp. 51–60, 2013.

[23] D. Bouayad and F. Emeriault, "Modeling the relationship between ground surface settlements induced by shield tunneling and the operational and geological parameters based on the hybrid PCA/ANFIS method," *Tunnelling and Underground Space Technology*, vol. 68, pp. 142–152, 2017.

[24] S. O. J. Jr and T. B. Celestino, "Artificial neural networks analysis of Sao Paulo subway tunnel settlement data," *Tunnelling and Underground Space Technology*, vol. 23, no. 5, pp. 481–491, 2008.

[25] M. Hasanipanah, M. Noorian-Bidgoli, A. D. Jahed, and H. Khamesi, "Feasibility of PSO-ANN model for predicting surface settlement caused by tunneling," *Engineering with Computers*, vol. 32, no. 4, pp. 705–715, 2016.

[26] W. Sun, M. Shi, C. Zhang, J. Zhao, and X. Song, "Dynamic load prediction of tunnel boring machine (TBM) based on heterogeneous in-situ data," *Automation in Construction*, vol. 92, pp. 23–34, 2018.

[27] S. Suwansawat and H. H. Einstein, "Artificial neural networks for predicting the maximum surface settlement caused by EPB shield tunneling," *Tunnelling and Underground Space Technology*, vol. 21, no. 2, pp. 133–150, 2006.

[28] A. Pourtaghi and M. A. Lotfollahi-Yaghin, "Wavenet ability assessment in comparison to ANN for predicting the maximum surface settlement caused by tunneling," *Tunnelling and Underground Space Technology*, vol. 28, pp. 257–271, 2012.

[29] V. R. Kohestani, M. R. Bazargan-Lari, and J. Asgari-marnani, "Prediction of maximum surface settlement caused by earth pressure balance shield tunneling using random forest," *Journal of Artificial Intelligence and Data Mining*, vol. 5, no. 1, pp. 127–135, 2017.

[30] R. P. Chen, P. Zhang, X. Kang, Z. Q. Zhong, Y. Liu, and H. N. Wu, "Prediction of maximum surface settlement caused by earth pressure balance (EPB) shield tunneling with ANN methods," *Soils and Foundations*, vol. 59, no. 2, pp. 284–295, 2019.

[31] J. Li, P. Li, D. Guo, X. Li, and Z. Chen, "Advanced prediction of tunnel boring machine performance based on big data," *Geoscience Frontiers*, vol. 12, no. 1, pp. 331–338, 2021.

[32] Z. Q. Liu, D. Guo, S. Lacasse, J. H. Li, B. B. Yang, and J. C. Choi, "Algorithms for intelligent prediction of landslide displacements," *Journal of Zhejiang University-SCIENCE A*, vol. 21, no. 6, pp. 412–429, 2020.

[33] D. Guo, J. Li, S. H. Jiang, X. Li, and Z. Chen, "Intelligent assistant driving method for tunnel boring machine based on big data," *Acta Geotechnica*, vol. 17, pp. 1019–1030, 2022.

[34] D. Guo, J. Li, X. Li, Z. Li, P. Li, and Z. Chen, "Advance prediction of collapse for TBM tunneling using deep learning method," *Engineering Geology*, vol. 299, article 106556, 2022.

[35] P. Vincent, H. Larochelle, I. Lajoie, Y. Bengio, P. A. Manzagol, and L. Bottou, "Stacked denoising autoencoders: learning useful representations in a deep network with a local denoising criterion," *The Journal of Machine Learning Research*, vol. 11, no. 12, pp. 3371–3408, 2010.

[36] B. B. Yang, K. L. Yin, S. Lacasse, and Z. Liu, "Time series analysis and long short-term memory neural network to predict landslide displacement," *Landslides*, vol. 16, no. 4, pp. 677–694, 2019.

[37] K. Cho, B. Van Merriënboer, C. Gulcehre et al., "Learning phrase representations using RNN encoder-decoder for statistical machine translation," in *Proceedings of the Conference on Empirical Methods in Natural Language Processing*pp. 1724–1734, Doha, 2014.

[38] L. Breiman, "Random forests," *Machine Learning*, vol. 45, no. 1, pp. 5–32, 2001.

[39] A. Liaw, M. Wiener, and A. Liaw, "Classification and regression by random forest," *R News*, vol. 2, pp. 18–21, 2002.

[40] S. M. Stigler, "Francis Galton's account of the invention of correlation," *Statistical Science*, vol. 4, no. 2, pp. 73–79, 1989.